Phase-specific manipulation of neural oscillations by transcranial alternating current stimulation

Marina Fiene[1], Bettina C. Schwab[1], Jonas Misselhorn[1], Christoph S. Herrmann[2,3], Till R. Schneider[1], Andreas K. Engel[1]

[1]Department of Neurophysiology and Pathophysiology, University Medical Center Hamburg-Eppendorf, Hamburg, Germany; [2]Experimental Psychology Lab, Department of Psychology, Cluster of Excellence "Hearing4all", European Medical School, Carl von Ossietzky University Oldenburg, Oldenburg, Germany; [3]Research Center Neurosensory Science, Carl von Ossietzky University Oldenburg, Oldenburg, Germany

Corresponding author

Marina Fiene

Department of Neurophysiology and Pathophysiology, University Medical Center Hamburg-Eppendorf

Martinistraße 52, 20246 Hamburg, Germany

Phone: +49 (0)40 7410-54680

Email: m.fiene@uke.de

Author contributions

M.F., B.C.S., J.M., C.S.H., T.R.S. and A.K.E. designed research; M.F. performed research; M.F. analyzed data; M.F. took lead in writing the manuscript; B.C.S. supervised data analysis and revised the manuscript. All authors contributed to discussion of data and the final version of the manuscript.

Keywords

transcranial alternating current stimulation (tACS), EEG, phase, alpha oscillations, visual flicker

Abstract

Oscillatory phase has been proposed as a key parameter defining the spatiotemporal structure of neural activity. To enhance our understanding of brain rhythms, phase-specific modulation of oscillations by transcranial alternating current stimulation (tACS) emerged as a promising approach. However, the effectiveness of tACS is still critically debated. Here, we investigated the phase-specificity of tACS effects on visually evoked steady state responses (SSRs). We observed that the phase shift between flicker and tACS modulates evoked SSR amplitudes. Neural sources of phase-specific effects were localized in the parieto-occipital cortex within flicker-aligned regions. Importantly, tACS effects were stronger in subjects with weaker locking of neural responses to flicker phase. Overall, our data provide evidence for a phase-specific modulation of oscillations by tACS, since SSR amplitude changes can only result from phase-dependent interactions with applied electric fields. This finding corroborates the physiological efficacy of tACS and highlights its potential for controlled modulations of brain signals.

Introduction

Oscillations are a prominent feature of activity in neural networks proposed to be of particular importance for neural processing and, by extension, for normal and pathological brain function (Engel et al., 2001; Fries, 2005; Ronconi et al., 2017; Schnitzler and Gross, 2005; Thut et al., 2012). The temporal patterning of neural activity has been related to the functional architecture of the brain and to communication between remote neural populations (Engel et al., 2001; Fries, 2005). Modulation of such cortical activity by means of non-invasive brain stimulation represents a promising approach to advance knowledge on the functional role of brain oscillations and to improve clinical outcomes in disorders related to aberrant neural activity. Specifically, transcranial alternating current stimulation (tACS) is widely applied in basic and clinical science with the aim to entrain neural activity, implying a periodic modulation of membrane potentials and a phase alignment of intrinsic oscillations to the tACS phase. This assumption is supported by in vitro slice preparations in rodents and recordings in primates showing phase-specific modulation of neuronal spiking patterns by externally applied electric fields (Ali et al., 2013; Krause et al., 2019; Reato et al., 2013). However, despite its broad use, the neural mechanism of tACS in the human brain is still under investigation and its efficacy has been challenged during recent years. Measurements of the electric field strength in human cadaver brains and epilepsy patients with implanted electrodes showed that most of the scalp-applied current is attenuated by skin and skull thereby questioning significant neural entrainment (Huang et al., 2017; Underwood, 2016; Vöröslakos et al., 2018). These findings were paralleled by inconsistent and stimulation frequency unspecific behavioral tACS effects (Brignani et al., 2013; Fekete et al., 2018; Vossen, 2017).

The theoretically ideal approach to directly measure tACS-induced phase-specific effects on oscillatory signals is complicated by strong, hard-to-predict electrical artifacts in concurrent recordings of neural activity. The application of routines to remove stimulation artifacts yielded contradictory results regarding the neural entrainment hypothesis (Helfrich et al., 2014a; Lafon et al., 2017; Strüber et al., 2014) and it is still questionable whether artifact removal techniques can reliably separate artifactual from brain activity (Noury et al., 2016; Noury and Siegel, 2017). To provide evidence for online phase-specific neuronal effects despite these methodological constraints, most studies assessed tACS effects on indirect measures assumed to be mediated by brain oscillations. For instance, tACS applied in the alpha and beta range was shown to lead to cyclic modulation of auditory, somatosensory or visual stimulus perception (Gundlach et al., 2016; Helfrich et al., 2014b; Neuling et al., 2012; Riecke et al., 2015). Further insight has been provided primarily in the motor domain, by showing tACS-phase-dependent

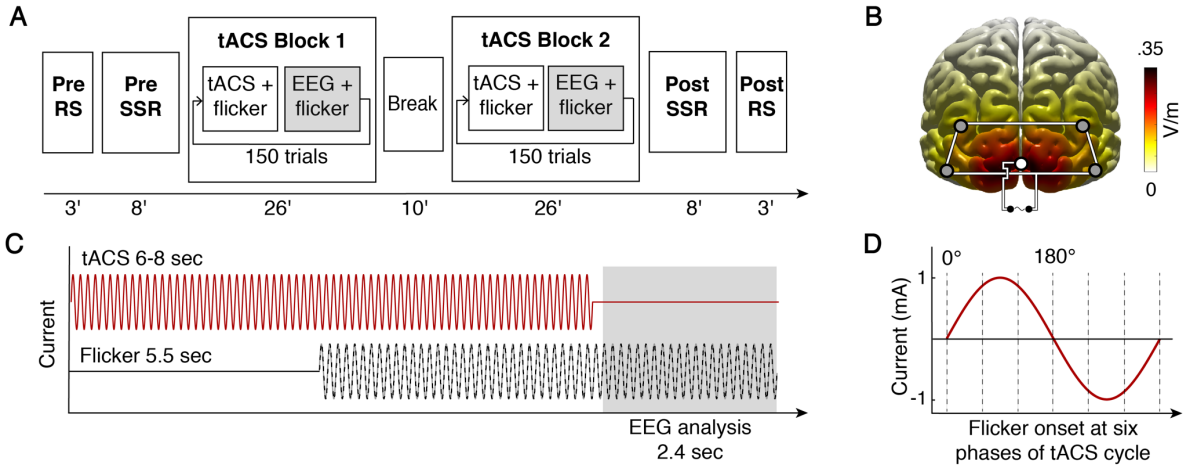

Figure 1. Experimental setup. (**A**) Schematic display of the experimental timeline. The experiment was conducted on two separate days for active tACS and sham stimulation. Resting state (RS) and visual evoked steady state response (SSR) data without tACS were recorded pre and post to the tACS blocks. (**B**) tACS electrode montage and power of the tACS-induced stimulation field. The occipital electrode montage induced highest current densities over the primary visual cortex and current spread in surrounding areas. Maximum peak-to-peak difference in field strength is about 0.7 V/m. (**C**) Illustration of one trial of the intermittent tACS protocol. Each trial started with tACS only, followed by flicker onset after 3-5 sec. The flicker continued for 5.5 sec until the end of the trial. tACS free intervals were used for EEG data analysis. (**D**) To vary the phase lag between activity induced by electrical and sensory rhythmic stimulation, visual flicker started at six different phase lags relative to the tACS cycle. 50 trials per phase angle were presented in randomized order.

changes in cortical excitability as measured by concurrent motor evoked potentials (Guerra et al., 2016; Nakazono et al., 2016; Schilberg et al., 2018) or tACS-induced enhancement and phase cancellation of peripheral tremor in healthy subjects and patients with Parkinson's disease by using closed-loop protocols (Bergmann et al., 2016; Brittain et al., 2013; Khatoun et al., 2018; Mehta et al., 2014). Yet, latest findings by Asamoah et al. (2019) revealed that tACS-effects on the motor cortex are dominated by cutaneous stimulation of peripheral nerves in the skin leading to rhythmic activation of the sensorimotor system rather than by transcranial modulation of cortical tissue. Thus, evidence for phase-specific effects of tACS in the motor domain might not necessarily be generalizable to transcranial entrainment effects in cortical regions apart from the motor cortex. Moreover, prior conclusions only hold true under the assumption that the chosen outcome measures, e.g. perception or cortical excitability, are reliable proxies for cortical oscillations.

Here, we used an innovative approach to directly target the phase-specificity of tACS effects on cortical oscillations via electroencephalography (EEG). To this end, we measured neural tACS effects on precisely controlled neuronal oscillations evoked by visual flicker, i.e., visual evoked steady state responses (SSRs). Compared to ongoing or task-related brain oscillations typically targeted in tACS research, flicker stimulation allows the precise control of the oscillatory phase in the visual cortex. Using an intermittent stimulation protocol, single trials of concurrent 10 Hz flicker and multi-electrode tACS over the primary visual cortex were applied in two sessions under active and sham tACS. Visual flicker was presented at six

different phase angles relative to the tACS cycle. Artifact free epochs in the immediate interval following tACS were used for EEG analysis of SSR amplitude as a function of phase lag between tACS and flicker stimulation (Figure 1). To account for overall changes in alpha amplitude over time, SSR amplitude per trial was computed as the difference between amplitude at the stimulation frequency (10 Hz) and the mean amplitude at neighboring frequencies (9 Hz; 11 Hz) using the Fourier Transform of time-domain EEG signals. We predicted that the systematically varied phase shift between flicker and tACS onset should modulate the amplitude of evoked SSRs.

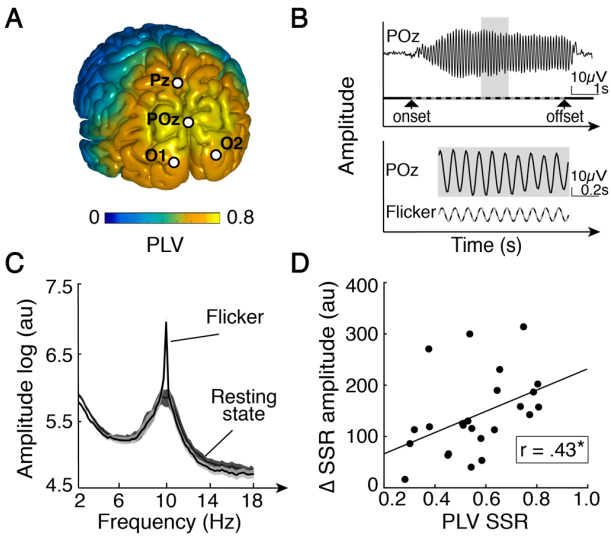

Figure 2. Phase locking values (PLVs) of steady state responses (SSRs) to flicker phase over all trials of the active and sham pre SSR blocks. (**A**) Spatial distribution of mean PLVs over all subjects showing maximal phase locking over the parieto-occipital cortex. Markers correspond to channels selected on sensor level for SSR amplitude analysis. (**B**) SSR during 5.5 sec flicker stimulation of one exemplary subject at channel POz (upper). Arrows mark the onset and offset of visual flicker. The enlarged data segment of the epoch highlighted in grey depicts constant phase locking to visual flicker (lower). (**C**) Mean amplitude spectrum during flicker stimulation and resting state over all subjects for the four selected channels on sensor level. Shaded areas indicate the standard error. (**D**) The strength of EEG-flicker PLV is positively correlated with the increase in SSR amplitude from resting state to flicker stimulation during pre SSR blocks across subjects. * $p < .05$.

Results

Flicker-evoked phase alignment in the parieto-occipital cortex. To check for sensory evoked flicker entrainment, we assessed the degree and spatial distribution of phase locking values (PLVs) between EEG and 10 Hz flicker stimulation. Estimated time series on source level displayed a prominent peak of parieto-occipital EEG-flicker PLV (Figure 2A). Strong phase locking was located in the superior and middle occipital gyrus as well as in bilateral precuneus and cuneus. For sensor level analysis, four parieto-occipital channels showing a population mean PLV > 0.5 (corresponding to electrodes O1, O2, POz, Pz) were selected for further analysis of SSR amplitude modulation by tACS. Mean PLV for the selected channels during both pre SSR blocks over all subjects was 0.56 ± 0.16 (mean ± sd). Amplitude spectra revealed an amplitude increase at the flicker stimulation frequency compared to resting state (Figure 2C). Between-subject correlation showed that the strength of PLV between EEG and flicker was positively correlated with the increase in SSR amplitude from resting state to pre SSR blocks ($r = .43$, $p = .04$) (Figure 2D).

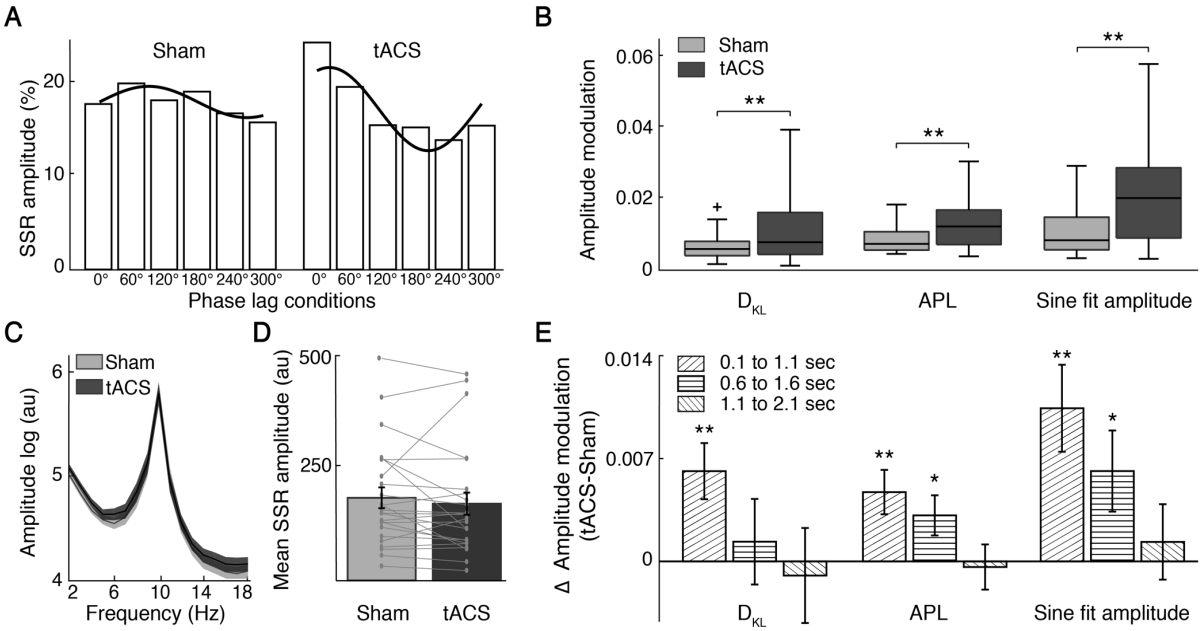

Figure 3. Steady state response (SSR) amplitude modulation by tACS shown for the time window of 0.1 to 1.1 sec after stimulation offset during the tACS block on sensor level. (**A**) SSR amplitude bar graphs for one exemplary subject. SSR amplitude values differ in the degree of phase dependence under tACS compared to sham. Black lines show sinusoidal fits to the data. (**B**) Significantly increased Kullback-Leibler divergence (D_{KL}), enhanced phase locking of amplitude values to phase condition (APL) and sine fit amplitudes under tACS relative to sham. (**C, D**) Phase-dependent amplitude modulation is not paralleled by differences in mean absolute 10 Hz alpha amplitude or mean SSR amplitude over all trials and subjects between stimulation conditions. Shaded areas and error bars indicate the standard error. (**E**) Decay in tACS effect size over three time windows after tACS offset. Bar graphs show the mean difference in SSR amplitude modulation between active and sham tACS condition quantified via three modulation measures. Asterisks mark the uncorrected *p*-value of dependent samples t-tests. Only statistical tests for the first 1 sec time epoch after tACS offset remain significant after Bonferroni correction for comparisons in multiple time windows (α_{bonf} = 0.0167; 0.05/3). Error bars represent the standard error. * $p < .05$; ** $p < .01$.

Phase-dependent SSR amplitude modulation by tACS. To test the hypothesis that simultaneous tACS and flicker stimulation lead to phase-specific interactions between evoked neural activity and electric field, we constructed bar diagrams of mean SSR amplitudes over the six phase lag conditions per subject (Figure 3A). The degree of tACS-phase-dependence of SSR amplitudes was assessed via (1) Kullback-Leibler divergence (D_{KL}), measuring the deviation of amplitude values from a uniform distribution, (2) the locking of amplitude values to phase conditions (amplitude phase locking, APL) and (3) one-cycle sine fit to SSR amplitude values. Thus, while D_{KL} describes a general modulation of SSR amplitudes, APL and sine fit assess systematic, phase-dependent modulation patterns. Figure 3A shows normalized SSR amplitude bar diagrams over the six phase lag conditions for one exemplary subject. During sham, data are almost uniformly distributed across phase bins, showing small fluctuations in SSR amplitude with no preference for a particular phase lag condition. On the contrary, the bar diagram for active stimulation shows phase-dependent modulations of SSR amplitudes indicating an interaction between tACS-induced electric field and flicker-evoked oscillatory activity. On sensor level, analysis of the deviation of amplitude values from uniform distribution revealed a significantly greater D_{KL} under tACS compared to sham within the first

1 sec epoch (0.1 to 1.1 sec) after tACS offset (t = -3.21, p = .004 < α_{bonf}) (Figure 3B). Phase locking of amplitude values to phase condition measured by APL was significantly larger after tACS (t = -3.12, p = .005 < α_{bonf}). In accordance, also the one-cycle sine wave fit to SSR amplitudes showed a significantly greater amplitude of the sine fit under tACS (t = -3.52, p = .002 < α_{bonf}) (Figure 3B). The proportion of explained variance R^2 by sine fit was greater for SSR amplitude modulation under tACS compared to sham (t = -2.65, p = .01). In successive time windows (0.6 to 1.6 sec; 1.1 to 2.1 sec), the modulatory tACS effect decayed for all three modulation parameters (p > α_{bonf}; Figure 3E). Importantly, the phase-dependent effects of tACS on SSR amplitude were not caused by overall 10 Hz alpha amplitude differences between conditions (Figure 3C). A repeated-measures t-test revealed no significant difference in mean SSR amplitude (t = 1.02, p = .32) over all trials per subject between tACS and sham condition during the first 1 sec interval after tACS offset (Figure 3D). Also, the standard deviation of SSR amplitude values over all trials per subject did not differ between sham and active stimulation condition (t = .31, p = .76). This implies a strengthening or dampening of SSR amplitudes dependent on the phase lag between flicker and tACS stimulation.

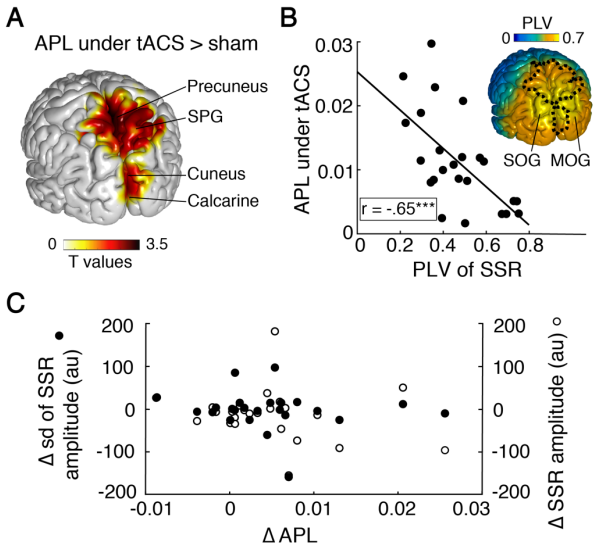

Figure 4. Analysis of tACS-induced amplitude phase locking (APL) of steady state responses (SSRs) during the first 1 sec epoch after tACS. (**A**): Significant differences in APL between active and sham tACS were localized in a cluster over the parieto-occipital cortex within flicker-aligned brain regions. (**B**): On sensor level, between-subject correlation shows that the tACS effect size quantified via APL is negatively related to EEG-flicker phase locking (PLV) during the tACS block. The insert illustrates that tACS effects (APL cluster boundary shown as dotted line) were mainly observed in regions where EEG-flicker PLVs did not peak during the tACS block. (**C**): The increase in APL values under tACS compared to sham was independent of overall changes in mean SSR amplitude or standard deviation (sd) of amplitude values over all trials per subject (sensor level data). MOG, middle occipital gyrus; SOG, superior occipital gyrus; SPG, superior parietal gyrus; *** p < .001.

Spatial localization and dependency of tACS effects on individual physiology. The spatial specificity of tACS effects was analyzed in source space for the APL modulation parameter. Compared to D_{KL}, APL is a more specific index assuming systematic amplitude modulations by tACS. Moreover, its computation is more stable compared to sine fit as no assumptions about parameter ranges are required. Cluster analysis in source space showed significantly increased APL values during active tACS relative to sham in a cluster over the parieto-occipital cortex (cluster test: p = .006) (Figure 4A). Significant differences were located primarily in the bilateral precuneus, superior parietal gyrus and midcingulate area as well as the cuneus and

calcarine sulcus. These are part of flicker-activated brain areas, located in tACS-targeted cortical regions and connected higher visual areas. Interestingly, tACS effects on SSR amplitude were not seen in the middle and superior occipital gyrus where neural phase alignment to the visual flicker peaked, but rather in neighboring occipital and parietal regions (insert in Figure 4B).

In accordance with this finding, we further observed a highly significant between-subject correlation of SSR amplitude modulation quantified by APL with individual EEG-flicker PLV during the active tACS block on sensor level (r = -.65, p < .001). Subjects with weaker PLV of SSR to flicker phase showed greater APL under tACS (Figure 4B). This relation was non-significant during the sham session (r = -.38, p = .07). Our results thus emphasize the impact of the individual physiology, influenced by the neuronal response strength to visual flicker, for the detection of neural tACS effects.

Importantly, the observed tACS effects did not significantly interact with the deviation of the applied tACS frequency from subjects' individual alpha frequency during resting state (see Figure 4 – figure supplement 1). Also, the increase in APL from sham to tACS could not be explained by a concurrent increase in mean SSR amplitude (r = -.22, p = .31) or standard deviation of SSR amplitude values (r = -.13, p = .56) over all trials of the tACS blocks per subject, thereby supporting the causal influence of the experimental manipulation of tACS-flicker phase lag (Figure 4C).

Discussion

Effects of tACS on oscillatory brain activity in humans are subject to ongoing debate. Here, we provide direct electrophysiological evidence for a phase-specific modulation of cortical oscillatory activity by tACS. The dependence of tACS effects on visually evoked SSR amplitude on the relative phase difference between sensory and electrical stimulation implies that tACS has a periodic impact on neuronal excitability. Importantly, we demonstrate a modulation of SSR amplitude for general as well as for cyclic, sinusoidal modulation measures. Source analysis locates effects within the parieto-occipital cortex and thus within flicker-aligned areas that were targeted by tACS. These results demonstrate the phase-specificity of tACS effects on cortical oscillations and thereby make an important contribution in the ongoing critical debate on tACS effects in humans.

The intermittent stimulation protocol and multi-electrode tACS montage chosen in the present study were effective in inducing neural aftereffects by short stimulation epochs of 6-8 sec. The modulatory effect on SSR amplitude was present during the first 1 sec interval after tACS offset

and was robust under three distinct modulation measures. However, phase-specific tACS effects already decayed after the first 1 sec time epoch. While lasting power enhancement after prolonged alpha tACS for up to 70 min has been repeatedly shown and ascribed to synaptic plasticity mechanisms (Kasten et al., 2016; Neuling et al., 2013; Vossen et al., 2015; Zaehle et al., 2010), evidence for outlasting effects on phase synchronization is still sparse. Assuming online phase-specific modulation of neural activity by tACS, Stonkus et al. (2016) hypothesized that oscillatory entrainment echoes can outlast the stimulation period for a few cycles (Hanslmayr et al., 2014; Stonkus et al., 2016). Accordingly, online entrainment by tACS might lead to post stimulation EEG activity phase locked to tACS offset. Using an intermittent tACS protocol with tACS epochs of 3 or 8 sec length, Vossen et al. (2015) demonstrated a general pre to post power increase at the stimulation frequency but no single trial prolonged phase locking of the EEG to the previous tACS signal. An important difference in the experimental setups between the study by Vossen et al. (2015) and our study is the combination of tACS with ongoing versus stimulus-evoked rhythmic brain activity. While tACS phase effects might not be detectable via PLV in ongoing brain activity, flicker-induced brain rhythms can increase the signal-to-noise ratio and might thereby enhance the detectability of tACS effects. Hypothesizing online periodic modulation of oscillatory activity and outlasting entrainment echoes to underlie our phase-dependent tACS effects on SSR amplitude, one can speculate that the modulatory effect might have even been stronger during tACS application.

Compared to ongoing or task-related brain oscillations typically targeted and taken as dependent variables in tACS research, SSRs allow the precise setting of oscillatory phase in the visual cortex. SSRs are recordable in the visual pathway at the flickering frequency with an amplitude maximum over the parieto-occipital cortex (Herrmann, 2001; Pastor et al., 2003). It is still debated whether SSRs describe a rhythmic repetition of evoked neural responses that add to ongoing brain activity or whether they actually reflect entrained intrinsic oscillations (Keitel et al., 2019; Notbohm et al., 2016). However, irrespective of their exact physiological origin, SSRs can be treated as stimulus-driven oscillations with predictable time course, which enables an ideal combination with rhythmic electrical stimulation by tACS. According to the above-mentioned neural phenomena underlying SSRs, the SSR amplitude modulation in our study could be explained by distinct neural mechanisms. On the one hand, tACS might be capable to phase-align intrinsic alpha oscillators and thereby induce additional synchronized oscillatory patterns that are phase-shifted relative to flicker-driven rhythmic activity. On the other hand, membrane potentials of neural populations driven by visual flicker could be concurrently influenced by electrical stimulation, thereby boosting or dampening neural

reactivity to flicker stimuli. Either way, our study results point to a phase-specific modulation of neural activity by tACS.

A critical methodological aspect in combining tACS with visual flicker is the relative phase lag between the stimulation waveforms of both methods. For at least two reasons, the phase lag between tACS and flicker-evoked cortical response may differ between subjects. First, flicker stimulation will inevitably lead to a variable delay in the recordable SSR due to individual conduction delays of the visual system. Second, depending on the interaction between the direction of the tACS electric field and individual anatomy, i.e., the orientation of cortical neurons in the stimulated region, tACS-induced neuromodulation may be shifted by half a stimulation cycle (Liu et al., 2018). Therefore, the optimal phase lag between flicker and tACS leading to an enhancement of SSR amplitude is expected to vary across subjects. This is in line with a recent study by Ruhnau et al. (2016a) showing that simultaneously started matched frequency tACS and flicker stimulation did not lead to tACS-induced power increase of the fundamental SSR component in the overall sample. In our study, the systematic phase lag variation between the two stimulation methods allowed for the investigation of net amplitude modulation over phase lag conditions individually for each subject. Post-hoc we could draw conclusions about the possibly optimal phase difference per participant. An alternative approach might be to first determine the individual SSR phase lag and to align tACS onset accordingly. While this procedure may allow the control of one potential source of variation, yet, tACS-phase effects would still vary between individuals depending on anatomical differences. Further, assuming a possible tACS-induced subthreshold shift in membrane potentials of flicker-activated neuronal populations, the optimal timing that boosts flicker responses does not necessarily correspond to in-phase sensory and electrical stimulation. Considering the limited knowledge on the physiological mechanisms of SSRs, our experimental design allowed to uncover phase-specific effects of tACS on cortical activity without reliance on pre-assumptions about the optimal phase delay.

Neural sites of tACS effects on flicker-driven oscillations were located within brain regions in the parieto-occipital cortex. These regions were part of the flicker-responsive areas as shown by the distribution of PLVs during flicker stimulation without tACS. On the one hand, our data show that tACS effects can not only be observed at early stages of the visual pathway directly affected by the electric field but also in more distant higher visual areas, i.e., the precuneus and superior parietal gyrus. This finding is in line with previous studies investigating the spatial distribution of tACS-effects and has been ascribed to polysynaptic interactions with the targeted population (Cabral-Calderin et al., 2016; Chai et al., 2018; Ozen et al., 2010). On the other

hand, our data suggest a contrary relation between the anatomical distribution of EEG-flicker PLVs and the localization of tACS effects. Distribution of PLVs of EEG to flicker showed maximal values over middle and superior occipital gyrus, cluster regions that showed less pronounced SSR modulation by tACS. Thus, tACS effects were especially prominent in visual areas that were not maximally driven by visual flicker. Also, our results demonstrate that tACS-induced SSR amplitude modulation was stronger in participants exposing weaker EEG-flicker PLV. Taken together, these findings emphasize a dependency of tACS effects on the individual physiology. It has previously been demonstrated that tACS effect sizes are related to the initial oscillatory activity level, meaning that effects were only measurable when power at the stimulated frequency was relatively low. For instance, under conditions of high endogenous alpha power, e.g., with eyes closed, alpha tACS failed to induce further power enhancement (Alagapan et al., 2016; Neuling et al., 2013; Ruhnau et al., 2016b). Similarly, our data indicate that in participants and in anatomical regions exhibiting strong EEG-flicker phase locking, the dominance of synchronous neural activity may have led to ceiling effects in alpha amplitude with no room for further enhancement. Besides alpha power ceiling effects, also the ratio between the strength of the external stimulation relative to the strength of the neural oscillation may be a critical factor for successful entrainment (Alagapan et al., 2016). As an alternative explanation, computational modeling studies proposed that the susceptibility of the neural system to external stimulation might depend on stochastic resonance and, thus, on the presence of irregular, asynchronous neural activity that amplifies the neural response to stimulation (Lefebvre et al., 2017). The presence of highly synchronized alpha oscillations might therefore have limited the subthreshold impact of the exogenous electric field on neural activity.

The mechanisms described above might not only affect the tACS efficacy but more generally also determine the degree of neural phase alignment to visual rhythmic stimulation. Interestingly, individual EEG-flicker PLV in the pre SSR blocks without tACS showed a moderate negative correlation with resting state alpha amplitude (r = -.41, p = .04; Figure 2 – figure supplement 1), indicating that limited entrainment related to high alpha levels occurred already in the absence of tACS. Thus, the current oscillatory activation level might have more general implications for the susceptibility of neural populations to externally induced neuromodulation. To further examine hypotheses on the dependency of electrical and sensory entrainment on individual physiology, a systematic variation in LED luminance could be used to assess the within-subject relation between baseline alpha amplitude, neuronal response properties measured by EEG-flicker PLV and tACS effect size.

Some methodological limitations also apply to our study. First, a double-blind design was not performed as we tracked the quality of the EEG signal during the intermittent stimulation protocol. The debriefing at the end of the second session showed that all but two participants were able to discriminate between sham and active sessions. However, this should not hamper the interpretation of our results, as field strengths were equivalent between phase lag conditions during active tACS which entails comparable sensations. Second, we cannot exclude a possible interaction between transcranial and cutaneous stimulation effects that might contribute to the observed phase-dependent SSR modulation. Stimulation of peripheral nerves in the skin might induce rhythmic activation in the somatosensory cortex. Cutaneous stimulation effects have been shown to largely explain tACS effects on motor cortex, however, it is unclear whether this explanation can be generalized to stimulation effects beyond motor cortex (Asamoah et al., 2019). In a recent study, we addressed this point by source analysis of neural effects induced by tACS over the parieto-occipital cortex (Schwab et al., 2019). The topographical localization of tACS effects in areas where current density of the electric field was strongest, i.e., the parieto-occipital cortex, speaks against a sole cutaneous effect underlying tACS neuromodulation. In future studies it needs to be examined how transcranial and cutaneous stimulation effects might interact depending on stimulation site, e.g., tACS over motor cortex or distant sensory brain regions. Last, we did not investigate the functional relation between changes in SSR amplitude and behavior. Whether SSR amplitude modulation has consequences for flicker perception, e.g., flicker luminance, remains subject to future studies.

In conclusion, we provide direct electrophysiological evidence for the efficacy of tACS to modulate cortical oscillatory activity in a phase-dependent manner. We found that the combination of tACS with sensory-evoked rhythmic brain activity leads to a phase-specific modulation of SSR amplitude. As the tACS mechanism of action is still unclear and its overall efficacy has recently been strongly debated, our findings emphasize the capability of tACS to periodically modulate neural activity in the human brain. This opens promising opportunities for the application of tACS to expand knowledge on the functional role of brain oscillations and the relevance of phase-synchronous activity for neural communication. Thus, our results have important implications for the clinical use of tACS to restore disturbed oscillatory activity and connectivity in brain disorders.

Materials and Methods

Participants. 24 healthy volunteers (mean age 25.1 ± 3.3 years; 16 female; 22 right-handed) were recruited from the University Medical Center Hamburg-Eppendorf, Germany. All participants reported normal or corrected-to-normal vision, no history of psychiatric or neurological disorders and were blind towards the tACS stimulation sequence. The experimental protocol was approved by the ethics committee of the Hamburg Medical Association and was conducted in accordance with the Declaration of Helsinki. All participants gave written informed consent before participation. Subjects were monetarily compensated and debriefed immediately after the experiment.

Experimental procedure. All subjects participated in two separate sessions in a randomized, counterbalanced order once under sham and active tACS. Participants were seated in a dimly lit, sound-attenuated EEG chamber at a distance of approximately 40 cm to a white light emitting diode (LED). Due to a nonlinear relation between forward voltage and luminosity of the used LED, we assessed LED luminosity per duty cycle of the pulse-width modulation by a luminance meter (LS-100, Konica Minolta). The resulting function was multiplied with a pure 10 Hz sine to generate a 10 Hz luminance signal. The LED had a maximal light intensity of 100 cd/m^2. Prior to the main tACS block, 3 min eyes-open resting state EEG (Pre RS) was recorded while subjects fixated the white illuminated LED. Afterwards, EEG during an 8 min SSR block without tACS (Pre SSR) was recorded. Single flicker periods (50 in total) were presented for 5.5 sec followed by short breaks of 3-5 sec. The timing of flicker presentation was identical to the procedure used in the main tACS block. In the tACS block, EEG was recorded continuously during the intermittent tACS protocol. Each trial started with tACS only and was followed by flicker onset after 3-5 sec. The flicker continued until the end of the trial for 5.5 sec in total. tACS free intervals of 2.5 sec were used for EEG data analysis. Single tACS periods had a duration of 6-8 sec. Between successive tACS epochs, tACS phase was continuous by adjusting only the amplitude but not the phase of the sine wave spanning the whole testing session. To account for the varying phase lag between neural activity induced by sensory and electrical stimulation, the visual flicker started at six different phase angles (0°, 60°, 120°, 180°, 240° and 300°) relative to the tACS cycle. 50 trials were recorded for each of the six phase lag conditions (300 trials in total). The sequence of trials was randomized such that every phase lag condition was followed equally likely by all other conditions. Moreover, to avoid confounding time-on-task effects on alpha amplitude, trials belonging to different conditions were evenly distributed over the course of the testing session by iterate permutation.

The tACS block was divided in two blocks interrupted by a 10 min break. After the tACS block, another SSR block without tACS (Post SSR) and resting state EEG (Post RS) were recorded. To ensure that subjects fixate the LED and thus to enhance SSR detection, participants were instructed to detect oddball trials in which LED luminance changed after 3-4 sec. Subjects responded per button press as soon as they detected a luminance change. 16 oddball trials were included in the tACS block and two oddball trials in the pre and post SSR blocks, respectively. Subjects showed a mean detection accuracy of 97.66 ± 9.99 % (mean ± sd) during the tACS blocks and 97.92 ± 12.39 % during the pre and post SSR blocks.

Electrophysiological recording. For electrophysiological recording, participants were seated in an electrically shielded chamber. EEG was recorded continuously from 64 Ag/AgCl electrodes (12 mm diameter) mounted in an elastic cap (Easycap). The EEG was referenced to the nose tip. The electrooculogram (EOG) was recorded from two electrodes placed below both eyes. Electrodes were prepared with abrasive conducting gel (Abralyt 2000, Easycap) keeping impedance below 20 kΩ. EEG data were recorded using BrainAmp DC amplifiers (Brain Products GmbH) and the corresponding software (Brain Products GmbH, Recorder 1.20). Data were recorded with an online passband of 0.016-250 Hz and digitized with a sampling rate of 1000 Hz.

tACS and electric field simulation. Multi-electrode tACS was applied via five additional Ag/AgCl electrodes (12 mm diameter) mounted between EEG electrodes. The montage was connected to a battery-driven current source (DC-Stimulator Plus, NeuroConn). After preparation with Signa electrolyte gel (Parker Laboratories Inc.), impedance of each outer electrode to the middle electrode was kept below 20 kΩ. Moreover, impedances were kept comparable to achieve an evenly distributed electric field. A sinusoidal alternating current of 2 mA peak-to-peak was applied at 10 Hz using an intermittent stimulation protocol. During sham and active stimulation, the current was ramped in over 15 sec to 2 mA. After 90 sec of continuous stimulation, tACS periods of 6-8 sec without ramp were applied interrupted by short breaks of 2.5 sec for EEG recording. Total stimulation time during the active session was 40 min. For sham stimulation, the current was ramped in and out over 15 sec each. This procedure ensured that in both stimulation conditions, participants experienced initial itching sensation. All subjects confirmed that stimulation was acceptable and did not induce painful skin sensations. The most common side-effect was a tingling feeling on the scalp under the electrode. During the debriefing at the end of the final session, except for two subjects all

participants correctly rated the sequence of active and sham stimulation. Further, we explored the experience of phosphenes during tACS in the beginning of each session. No participant reported perceived phosphenes. This finding is in line with our simulation of the tACS-induced electric field which greatly diminishes with increasing distance to stimulation electrodes and is expected to be low in the retina.

Placement of tACS electrodes was chosen to target brain regions activated by visual stimulation. We aimed to achieve largest magnitudes of current density in the primary visual cortex to maximally interfere with early stages of cortical sensory processing. Quantitative field distributions $\vec{E}$ could directly be computed by linear superposition of lead fields $\vec{L}$, weighted by the injected currents α_i at electrodes $i = \{1,2,3,4,5\}$:

$$\vec{E}(\vec{x}) = \sum_i (\overrightarrow{L_i}(\vec{x})\ \alpha_i)$$

$\vec{L}$ was estimated with the boundary element method using a volume conduction model by Oostenveld et al. (2003) at 5 mm spatial resolution.

Data analysis

Data preprocessing. 64-channel EEG data were preprocessed and analyzed in Matlab (The MathWorks Inc.) using the analysis toolbox FieldTrip (Oostenveld et al., 2011). Circular statistics were calculated with the CircStat toolbox (Berens, 2009). EEG recordings during the pre and post SSR blocks without tACS were segmented into epochs from -1.5 to 6.5 sec around flicker onset. For the tACS block, EEG was segmented into epochs from 0.1 to 2.5 sec after tACS offset. The first 0.1 sec after stimulation offset were rejected before filtering to avoid leakage of tACS artifacts. EEG data were bandpass filtered from 1 to 20 Hz using a Hamming-windowed sinc FIR filter. Oddball trials and trials during which participants erroneously responded via button press were excluded. To automatically screen for high noise level electrodes, channels whose standard deviation exceeded 3 times the median standard deviation of all channels per subject were excluded. On average, 4.0 ± 1.9 channels were removed. Data were downsampled to 100 Hz. Afterwards, independent component analysis (ICA) was computed using the infomax ICA algorithm (Bell and Sejnowski, 2002). Remaining eye-movement, cardiac and noise artifacts were removed based on visual inspection of the components' time course, spectrum and topography. For eye-blink artifact removal, Pearson linear correlation coefficient between EOG and ICA components was calculated and components showing correlation coefficients greater than .25 were rejected. On average, 20.1 ± 3.9 components were excluded. Finally, all trials were visually inspected and trials

containing artifacts that had not been detected by previous steps were manually removed. On average, 49.19 ± 1.2 out of 50 trials remained for the pre and post SSR blocks and 296.9 ± 3.5 out of 300 trials remained for the tACS block per subject.

Source reconstruction. At the cortical source level, neural activity was estimated using exact low resolution brain electromagnetic tomography (eLORETA). Before source projection, data were bandpass filtered between 7-13 Hz with a 4th order butterworth filter. The cortical grid was defined using the Automated Anatomical Labeling (AAL) atlas consisting of 38 regions after excluding subcortical and cerebellar structures (Hahm et al., 2017). Three-dimensional time series were estimated in a linearly spaced grid of 4077 cortical points with 7.5 mm distance in all three spatial directions using the boundary element method volume conduction model by Oostenveld et al. (2003). eLORETA was applied per trial with 5% regularization. To reduce spatial dimensions, the three resulting time series were projected to the direction of maximal power at each grid point.

Spectral analysis and SSR amplitude modulation indices. EEG spectral analysis was performed on sensor and source level. We expected to find tACS-induced modulations of SSR amplitude at electrode positions showing a clear response to visual flicker, i.e., where phase alignment to flicker stimulation is prominent. Therefore, we assessed the spatial distribution of phase locking of EEG to visual flicker in the pre SSR blocks without tACS for the sham and active tACS testing session. A Hilbert transform was computed on the flicker signal and EEG time series during flicker stimulation (1.0 to 5.5 sec after flicker onset) for each trial at each electrode and voxel. The first 1 sec after flicker onset was removed to ensure the SSR has fully build up. To assess phase stability, the time-dependent differences in phase signals ($\phi_{flicker}(t) - \phi_{EEG}(t)$) were computed and the extent of entrainment quantified by the phase locking value (PLV) over all trials.

$$PLV = \left| \frac{1}{N_{trials}} \sum_{k=1}^{N_{trials}} \left(\frac{1}{N_{time}} \sum_{t=1}^{N_{time}} e^{i(\phi_{flicker}(t) - \phi_{EEG}(t))} \right) \right|$$

For sensor level analysis, we selected those channels showing prominent phase entrainment with mean PLV > 0.5 over all subjects. Correlation between PLV and SSR amplitude increase from resting state to pre SSR blocks was quantified by computing a Pearson correlation coefficient. SSR amplitude was calculated according to the A_{SSR} formula (see below) on 1 sec

time windows with an overlap of 0.5 sec for each 3 min resting state block (pre RS) and for each 4.5 sec trial of the pre SSR blocks.

For analysis of SSR amplitude modulation during the tACS block, we computed the Fourier transform of each trial separately for the time epochs of 0.1 to 1.1 sec, 0.6 to 1.6 sec and 1.1 to 2.1 sec after tACS offset. To correct for global alpha amplitude fluctuations over time independent of experimental manipulation, the SSR amplitude A_{SSR} was computed as a relative amplitude value by subtracting the mean amplitude at neighboring frequencies (9 and 11 Hz) from the absolute amplitude A_{10Hz} at the stimulation frequency.

$$A_{SSR} = A_{10Hz} - (A_{9Hz} + A_{11Hz})/2$$

To assess modulation of SSR amplitude dependent on the relative phase lag between tACS and flicker onset, we constructed bar diagrams showing the variation in SSR amplitude over phase lag conditions. SSR amplitude was normalized by the sum of amplitude values over all six conditions. If there was no phase-specific amplitude modulation by concurrent tACS, bar graphs should be uniformly distributed. In case of phase-specific interactions, the SSR amplitude should be higher in a condition that shows an optimal phase lag for that subject. Assuming that the optimal phase lag between flicker and tACS onset leading to increased SSR amplitudes might vary between subjects, any preference in phase lag condition compared to sham can be considered as evidence for phase specific tACS entrainment. Amplitude modulation was quantified by three modulation measures. First, we calculated the Kullback-Leibler divergence (D_{KL}) which is a common premetric used in statistics to calculate the amount of difference between two distributions. The deviation of the observed amplitude distribution P from the uniform distribution U is defined as

$$D_{KL}(P,U) = \sum_{i=1}^{N} P(i)\, log\left[\frac{P(i)}{U(i)}\right]$$

where N is the number of phase bins (Tort et al., 2010). Strict uniformly distributed amplitude values would be reflected in $D_{KL} = 0$ whereas D_{KL} increases the further away P gets from U. While D_{KL} measures the overall deviation of amplitude values from uniform distribution, we additionally assessed whether the tACS-induced amplitude modulation over phase conditions follows a cyclic pattern, as hypothesized based on the sinusoidal nature of the tACS signal. Therefore, we calculated the phase locking value of amplitude values to phase condition. This cyclic amplitude phase locking (APL) index is defined as

$$APL = \left| \sum_{b} A_b \, e^{i\theta b} \right|$$

where A and θ are the normalized relative amplitude and phase lag for each of the six phase lag conditions b. To further investigate whether the tACS-induced SSR amplitude modulation can be described by a sinusoidal pattern, we fitted one-cycle sine waves to SSR amplitude bar diagram values (Neuling et al., 2012; Wilsch et al., 2018). The following equation was fit to the six normalized SSR amplitude values per subject and stimulation condition.

$$y = b + a * \sin\left(10Hz * 2\pi * x \; + \; c\right)$$

where x corresponds to the flicker-tACS phase lags during one cycle (x = {0, 1/6T, 2/6T,… 5/6∗T} with period T = 0.1 sec). The parameters a, b and c were estimated by the fitting procedure where b is the intercept, a the amplitude and c the phase shift. Parameters a and b were bound between -1 and 1 and c between 0 and 2π. Start values were drawn randomly from within the range of restrictions for each parameter. Model fits were computed using the Matlab fittype function allowing for 1000 iterations to find the best model. We examined the absolute sine fit amplitude values as index for the strength of SSR amplitude modulation. The significance of the sine fit was assessed by dependent samples t-tests comparing the proportion of explained variance R^2 as goodness-of-fit index between sham and active tACS session.

For each of the three modulation indices, we calculated dependent samples t-tests for the epochs of 0.1 to 1.1 sec, 0.6 to 1.6 sec and 1.1 to 2.1 sec after tACS offset between sham and active tACS on sensor level. To account for comparisons in multiple time windows, we applied Bonferroni correction to the significance level and report test statistics if the corresponding p-value fell below the corrected alpha of α_{bonf} = .0167 (= .05/3). Interrelation between modulation measures were assessed by Pearson correlation coefficients.

For further investigation of tACS effects, we analyzed the APL parameter resulting from the epoch immediately following tACS offset in source space. APL is the more specific, phase-dependent modulation index relative to D_{KL} and a more robust measure not requiring any presuppositions on parameter ranges as compared to sine fit. For source localization of APL effects, dependent samples t-tests were computed for each voxel. We performed cluster-based permutation tests to correct for multiple comparisons problem. Clusters were obtained by summing up t-values which were adjacent in space and below an alpha level of 5 % (two-sided). A permutation distribution was generated by randomly shuffling APL values between active and sham condition within subjects in each of 1000 iterations. The observed cluster was considered statistically significant when the sum of t-values exceeded 95 % of the permutation

distribution. To further examine whether the strength of tACS effects quantified by APL is dependent on subjects' response to flicker stimulation, we assessed Pearson correlation coefficients between APL and EEG-flicker PLV for sham and active tACS blocks. Moreover, we assessed the dependency of the increase in APL from sham to tACS on the change in mean SSR amplitude or the standard deviation of SSR amplitudes over all trials per subject by computing Pearson correlation coefficients.

Acknowledgements

This work was supported by the Deutsche Forschungsgemeinschaft (SFB 936/A3 and SPP 1665/EN 533/13-1 awarded to A.K.E.; SPP 1665/SCHN 1511/1-2 awarded to T.R.S.). We thank Jonathan Daume, Alexander Maye, Jan-Ole Radecke and Darius Zokai for helpful discussions on the data, Malte Sengelmann and Guido Nolte for methodological support, and Karin Deazle and Darius Zokai for assistance in data recording.

Conflict of interest

The authors declare that no competing interests exist.

References

Alagapan S, Schmidt SL, Lefebvre J, Hadar E, Shin HW, Fröhlich F. 2016. Modulation of cortical oscillations by low-frequency direct cortical stimulation is state-dependent. *PLOS Biology* **14**:e1002424. doi:10.1371/journal.pbio.1002424

Ali MM, Sellers KK, Fröhlich F. 2013. Transcranial alternating current stimulation modulates large-scale cortical network activity by network resonance. *Journal of Neuroscience* **33**:11262–11275. doi:10.1523/JNEUROSCI.5867-12.2013

Asamoah B, Khatoun A, Mc Laughlin M. 2019. tACS motor system effects can be caused by transcutaneous stimulation of peripheral nerves. *Nature Communications* **10**:266. doi:10.1038/s41467-018-08183-w

Bell AJ, Sejnowski TJ. 2002. Blind separation and blind deconvolution: An information-theoretic approach **5**:3415–3418. doi:10.1109/ICASSP.1995.479719

Berens P. 2009. CircStat: A MATLAB toolbox for circular statistics. *Journal of Statistical Software* **31**:1–21.

Bergmann TO, Karabanov A, Hartwigsen G, Thielscher A, Siebner HR. 2016. Combining non-invasive transcranial brain stimulation with neuroimaging and electrophysiology: Current approaches and future perspectives. *NeuroImage* **140**:4–19. doi:10.1016/j.neuroimage.2016.02.012

Brignani D, Ruzzoli M, Mauri P, Miniussi C. 2013. Is transcranial alternating current stimulation effective in modulating brain oscillations? *PLoS ONE* **8**:e56589. doi:10.1371/journal.pone.0056589

Brittain J-S, Probert-Smith P, Aziz TZ, Brown P. 2013. Tremor suppression by rhythmic transcranial current stimulation. *Current Biology* **23**:436–440. doi:10.1016/j.cub.2013.01.068

Cabral-Calderin Y, Anne Weinrich C, Schmidt-Samoa C, Poland E, Dechent P, Bähr M, Wilke M. 2016. Transcranial alternating current stimulation affects the BOLD signal in a frequency and task-dependent manner. *Human Brain Mapping* **37**:94–121. doi:10.1002/hbm.23016

Chai Y, Sheng J, Bandettini PA, Gao J-H. 2018. Frequency-dependent tACS modulation of BOLD signal during rhythmic visual stimulation. *Human Brain Mapping* **39**:2111–2120. doi:10.1002/hbm.23990

Engel AK, Fries P, Singer W. 2001. Dynamic predictions: Oscillations and synchrony in top–down processing. *Nature Reviews Neuroscience* **2**:704–716. doi:10.1038/35094565

Fekete T, Nikolaev AR, De Knijf F, Zharikova A, van Leeuwen C. 2018. Multi-electrode

alpha tACS during varying background tasks fails to modulate subsequent alpha power. *Frontiers in Neuroscience* **12**:428. doi:10.3389/fnins.2018.00428

Fries P. 2005. A mechanism for cognitive dynamics: Neuronal communication through neuronal coherence. *Trends in Cognitive Sciences* **9**:474–480. doi:10.1016/j.tics.2005.08.011

Guerra A, Pogosyan A, Nowak M, Tan H, Ferreri F, Di Lazzaro V, Brown P. 2016. Phase dependency of the human primary motor cortex and cholinergic inhibition cancelation during beta tACS. *Cerebral Cortex* **26**:3977–3990. doi:10.1093/cercor/bhw245

Gundlach C, Müller MM, Nierhaus T, Villringer A, Sehm B. 2016. Phasic modulation of human somatosensory perception by transcranially applied oscillating currents. *Brain Stimulation* **9**:712–719. doi:10.1016/j.brs.2016.04.014

Hahm J, Lee H, Park H, Kang E, Kim YK, Chung CK, Kang H, Lee DS. 2017. Gating of memory encoding of time-delayed cross-frequency MEG networks revealed by graph filtration based on persistent homology. *Scientific Reports* **7**:41592. doi:10.1038/srep41592

Hanslmayr S, Matuschek J, Fellner M-C. 2014. Entrainment of prefrontal beta oscillations induces an endogenous echo and impairs memory formation. *Current Biology* **24**:904–909. doi:10.1016/j.cub.2014.03.007

Helfrich RF, Knepper H, Nolte G, Strüber D, Rach S, Herrmann CS, Schneider TR, Engel AK. 2014a. Selective modulation of interhemispheric functional connectivity by HD-tACS shapes perception. *PLoS Biology* **12**:e1002031. doi:10.1371/journal.pbio.1002031

Helfrich RF, Schneider TR, Rach S, Trautmann-Lengsfeld SA, Engel AK, Herrmann CS. 2014b. Entrainment of brain oscillations by transcranial alternating current stimulation. *Current Biology* **24**:333–339. doi:10.1016/j.cub.2013.12.041

Herrmann CS. 2001. Human EEG responses to 1-100 Hz flicker: Resonance phenomena in visual cortex and their potential correlation to cognitive phenomena. *Experimental Brain Research* **137**:346–353. doi:10.1007/s002210100682

Huang Y, Liu AA, Lafon B, Friedman D, Dayan M, Wang X, Bikson M, Doyle WK, Devinsky O, Parra LC. 2017. Measurements and models of electric fields in the in vivo human brain during transcranial electric stimulation. *eLife* **6**:1–26. doi:10.7554/eLife.18834

Kasten FH, Dowsett J, Herrmann CS. 2016. Sustained aftereffect of α-tACS lasts up to 70 min after stimulation. *Frontiers in Human Neuroscience* **10**:1–9. doi:10.3389/fnhum.2016.00245

Keitel C, Keitel A, Benwell CS, Daube C, Thut G, Gross J. 2019. Stimulus-driven brain rhythms within the alpha band: The attentional-modulation conundrum. *The Journal of Neuroscience* 1633–18. doi:10.1523/JNEUROSCI.1633-18.2019

Khatoun A, Breukers J, Op de Beeck S, Nica IG, Aerts J-M, Seynaeve L, Haeck T, Asamoah B, Mc Laughlin M. 2018. Using high-amplitude and focused transcranial alternating current stimulation to entrain physiological tremor. *Scientific Reports* **8**:8221. doi:10.1038/s41598-018-26013-3

Krause MR, Vieira PG, Csorba BA, Pilly PK, Pack CC. 2019. Transcranial alternating current stimulation entrains single-neuron activity in the primate brain. *Proceedings of the National Academy of Sciences* 201815958. doi:10.1073/pnas.1815958116

Lafon B, Henin S, Huang Y, Friedman D, Melloni L, Thesen T, Doyle W, Buzsáki G, Devinsky O, Parra LC, A. Liu A. 2017. Low frequency transcranial electrical stimulation does not entrain sleep rhythms measured by human intracranial recordings. *Nature Communications* **8**:1199. doi:10.1038/s41467-017-01045-x

Lefebvre J, Hutt A, Fröhlich F. 2017. Stochastic resonance mediates the state-dependent effect of periodic stimulation on cortical alpha oscillations. *eLife* **6**:1–21. doi:10.7554/eLife.32054

Liu A, Vöröslakos M, Kronberg G, Henin S, Krause MR, Huang Y, Opitz A, Mehta A, Pack CC, Krekelberg B, Berényi A, Parra LC, Melloni L, Devinsky O, Buzsáki G. 2018. Immediate neurophysiological effects of transcranial electrical stimulation. *Nature Communications* **9**:5092. doi:10.1038/s41467-018-07233-7

Mehta AR, Brittain J-S, Brown P. 2014. The selective influence of rhythmic cortical versus cerebellar transcranial stimulation on human physiological tremor. *Journal of Neuroscience* **34**:7501–7508. doi:10.1523/JNEUROSCI.0510-14.2014

Nakazono H, Ogata K, Kuroda T, Tobimatsu S. 2016. Phase and frequency-dependent effects of transcranial alternating current stimulation on motor cortical excitability. *PLOS ONE* **11**:e0162521. doi:10.1371/journal.pone.0162521

Neuling T, Rach S, Herrmann CS. 2013. Orchestrating neuronal networks: Sustained after-effects of transcranial alternating current stimulation depend upon brain states. *Frontiers in Human Neuroscience* **7**:161. doi:10.3389/fnhum.2013.00161

Neuling T, Rach S, Wagner S, Wolters CH, Herrmann CS. 2012. Good vibrations: Oscillatory phase shapes perception. *NeuroImage* **63**:771–778. doi:10.1016/j.neuroimage.2012.07.024

Notbohm A, Kurths J, Herrmann CS. 2016. Modification of brain oscillations via rhythmic

light stimulation provides evidence for entrainment but not for superposition of event-related responses. *Frontiers in Human Neuroscience* **10**:10. doi:10.3389/fnhum.2016.00010

Noury N, Hipp JF, Siegel M. 2016. Physiological processes non-linearly affect electrophysiological recordings during transcranial electric stimulation. *NeuroImage* **140**:99–109. doi:10.1016/j.neuroimage.2016.03.065

Noury N, Siegel M. 2017. Phase properties of transcranial electrical stimulation artifacts in electrophysiological recordings. *NeuroImage* **158**:406–416. doi:10.1016/j.neuroimage.2017.07.010

Oostenveld R, Fries P, Maris E, Schoffelen J-M. 2011. FieldTrip: Open source software for advanced analysis of MEG, EEG, and invasive electrophysiological data. *Computational Intelligence and Neuroscience* **2011**:1–9. doi:10.1155/2011/156869

Oostenveld R, Stegeman DF, Praamstra P, van Oosterom A. 2003. Brain symmetry and topographic analysis of lateralized event-related potentials. *Clinical Neurophysiology* **114**:1194–1202. doi:10.1016/S1388-2457(03)00059-2

Ozen S, Sirota A, Belluscio MA, Anastassiou CA, Stark E, Koch C, Buzsaki G. 2010. Transcranial electric stimulation entrains cortical neuronal populations in rats. *Journal of Neuroscience* **30**:11476–11485. doi:10.1523/JNEUROSCI.5252-09.2010

Pastor MA, Artieda J, Arbizu J, Valencia M, Masdeu JC. 2003. Human cerebral activation during steady-state visual-evoked responses. *The Journal of neuroscience : the official journal of the Society for Neuroscience* **23**:11621–11627. doi:23/37/11621 [pii]

Reato D, Rahman A, Bikson M, Parra LC. 2013. Effects of weak transcranial alternating current stimulation on brain activity—a review of known mechanisms from animal studies. *Frontiers in Human Neuroscience* **7**:687. doi:10.3389/fnhum.2013.00687

Riecke L, Formisano E, Herrmann CS, Sack AT. 2015. 4-Hz transcranial alternating current stimulation phase modulates hearing. *Brain Stimulation* **8**:777–783. doi:10.1016/j.brs.2015.04.004

Ronconi L, Oosterhof NN, Bonmassar C, Melcher D. 2017. Multiple oscillatory rhythms determine the temporal organization of perception. *Proceedings of the National Academy of Sciences* **114**:13435–13440. doi:10.1073/pnas.1714522114

Ruhnau P, Keitel C, Lithari C, Weisz N, Neuling T. 2016a. Flicker-driven responses in visual cortex change during matched-frequency transcranial alternating current stimulation. *Frontiers in Human Neuroscience* **10**:184. doi:10.3389/fnhum.2016.00184

Ruhnau P, Neuling T, Fuscá M, Herrmann CS, Demarchi G, Weisz N. 2016b. Eyes wide shut:

Transcranial alternating current stimulation drives alpha rhythm in a state dependent manner. *Scientific Reports* **6**:27138. doi:10.1038/srep27138

Schilberg L, Engelen T, ten Oever S, Schuhmann T, de Gelder B, de Graaf TA, Sack AT. 2018. Phase of beta-frequency tACS over primary motor cortex modulates corticospinal excitability. *Cortex* **103**:142–152. doi:10.1016/j.cortex.2018.03.001

Schnitzler A, Gross J. 2005. Normal and pathological oscillatory communication in the brain. *Nature Reviews Neuroscience* **6**:285–296. doi:10.1038/nrn1650

Schwab BC, Misselhorn J, Engel AK. 2019. Modulation of large-scale cortical coupling by transcranial alternating current stimulation. *Brain Stimulation*. doi:10.1016/j.brs.2019.04.013

Stonkus R, Braun V, Kerlin JR, Volberg G, Hanslmayr S. 2016. Probing the causal role of prestimulus interregional synchrony for perceptual integration via tACS. *Scientific Reports* **6**:32065.

Strüber D, Rach S, Trautmann-Lengsfeld SA, Engel AK, Herrmann CS. 2014. Antiphasic 40 Hz oscillatory current stimulation affects bistable motion perception. *Brain Topography* **27**:158–171. doi:10.1007/s10548-013-0294-x

Thut G, Miniussi C, Gross J. 2012. The functional importance of rhythmic activity in the brain. *Current Biology* **22**:R658–R663. doi:10.1016/j.cub.2012.06.061

Tort ABL, Komorowski R, Eichenbaum H, Kopell N. 2010. Measuring phase-amplitude coupling between neuronal oscillations of different frequencies. *Journal of Neurophysiology* **104**:1195–1210. doi:10.1152/jn.00106.2010

Underwood E. 2016. Cadaver study challenges brain stimulation methods. *Science* **352**:397–397. doi:10.1126/science.352.6284.397

Vöröslakos M, Takeuchi Y, Brinyiczki K, Zombori T, Oliva A, Fernández-Ruiz A, Kozák G, Kincses ZT, Iványi B, Buzsáki G, Berényi A. 2018. Direct effects of transcranial electric stimulation on brain circuits in rats and humans. *Nature Communications* **9**:483. doi:10.1038/s41467-018-02928-3

Vossen A. 2017. Modulation of neural oscillations and associated behaviour by transcranial alternating current stimulation (tACS). PhD thesis.

Vossen A, Gross J, Thut G. 2015. Alpha power increase after transcranial alternating current stimulation at alpha frequency (α-tACS) reflects plastic changes rather than entrainment. *Brain Stimulation* **8**:499–508. doi:10.1016/j.brs.2014.12.004

Wilsch A, Neuling T, Obleser J, Herrmann CS. 2018. Transcranial alternating current stimulation with speech envelopes modulates speech comprehension. *NeuroImage*

172:766–774. doi:10.1016/j.neuroimage.2018.01.038

Zaehle T, Rach S, Herrmann CS. 2010. Transcranial alternating current stimulation enhances individual alpha activity in human EEG. *PLoS ONE* **5**:e13766. doi:10.1371/journal.pone.0013766

Figure supplements

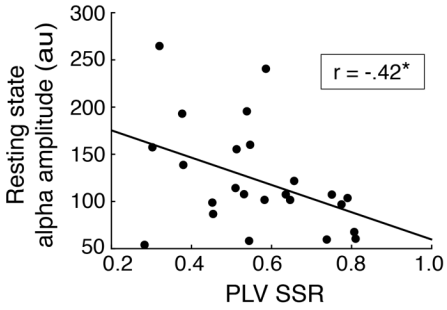

Figure 2 – figure supplement 1. Correlation between resting state alpha amplitude and phase-locking value (PLV) of the flicker-evoked steady state response (SSR) to flicker phase for the active and sham tACS sessions. For quantification of resting state alpha, mean amplitude spectra of non-overlapping 1 sec epochs during the 3 min pre resting state (pre RS) blocks were estimated. Alpha amplitude was defined as the mean amplitude in the range of 8-12 Hz for the four parieto-occipital electrodes (O1, O2, POz, Pz). The Pearson correlation coefficient between resting state alpha amplitude and EEG-flicker PLV during pre SSR blocks is $r = -.42$, $p = .04$. * $p < .05$.

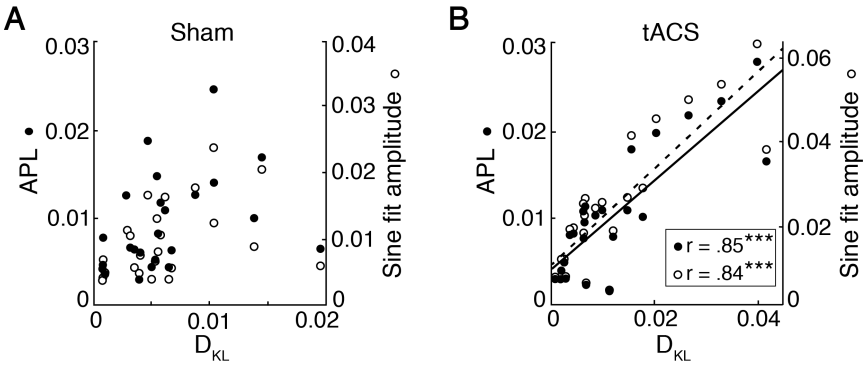

Figure 3 – figure supplement 1. Correlation of amplitude modulation parameters for the time window of 0.1 to 1.1 sec after stimulation offset during the sham and active tACS block on sensor level. (**A**) Under sham, data show a marginal positive correlation (DKL and APL $r = .39$, $p = .06$; DKL and sine fit amplitude $r = .38$, $p = .07$). This tendency is expectable und would also apply to variation in noise data. (**B**) Under tACS, modulation parameters were highly positively correlated. With stronger tACS-induced deviation from uniform distribution measured by D_{KL}, amplitude values increasingly followed a phase-dependent modulation pattern. The solid line depicts the correlation between D_{KL} and APL, the dashed line displays the correlation between D_{KL} and sine fit amplitude. APL, phase locking of amplitude values to phase condition, D_{KL}, Kullback-Leibler divergence; *** $p < .001$.

750

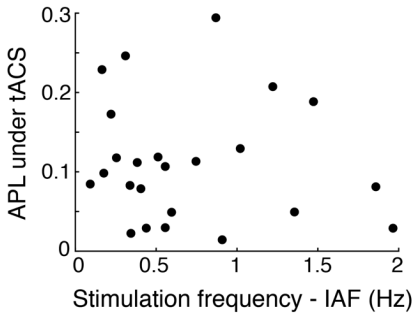

Figure 4 – figure supplement 1. No dependence of SSR amplitude modulation under tACS quantified by APL on the deviation of the stimulation frequency (10 Hz) from the individual alpha frequency (IAF). For IAF determination, the amplitude spectrum was estimated for the 3 min pre resting state (pre RS) data of the tACS session. Amplitudes were averaged for the four parieto-occipital electrodes (O1, O2, POz, Pz). The IAF was defined as the peak frequency within the alpha range of 8-12 Hz. The Pearson correlation of APL with the difference between stimulation frequency and IAF is $r = -0.09$, $p = .66$.